ACS SENSORS

pubs.acs.org/acssensors

Article

Distance-Based Biosensor for Ultrasensitive Detection of Uracil-DNA Glycosylase Using Membrane Filtration of DNA Hydrogel

Chao Jiang, Fangfang Wang, Kexin Zhang, Tiantian Min, Desheng Chen, and Yongqiang Wen*

Cite This: *ACS Sens.* 2021, 6, 2395−2402

Read Online

ACCESS | Metrics & More | Article Recommendations | Supporting Information

ABSTRACT: In the deoxyribonucleic acid (DNA) repair pathways, DNA repair enzymes have great significance for genomic integrity. As one important initiator of the base-excision repair pathway, the aberrant activity of uracil-DNA glycosylase (UDG) is closely associated with many diseases. Herein, we developed a simple distance-based device for visual detection of UDG activity using a load-free DNA hydrogel. The DNA hydrogel consists of polyacrylamide−DNA chains being bridged by a single-stranded DNA crosslinker containing a responsive uracil base site. UDG can recognize and remove the uracil, resulting in the cleavage effect of the DNA crosslinker strand with the assistance of endonuclease IV (Endo IV). Plugging one end of the capillary tube, the DNA hydrogel acting as a filter membrane separator would control molecules to flow into the tube. The integrity of the DNA hydrogel networks is affected by the excision of UDG. Therefore, taking full advantage of membrane filtration of the DNA hydrogel, the activity of UDG can be quantitatively detected via reading the distance of the red indicator solution in the capillary tube. Without any instruments and complicated procedures, this method realizes high sensitivity and specificity for the detection of UDG as low as 0.02 mU/mL and can even measure UDG in complex cell samples. Additionally, this method is simple, universal, and can be used to screen inhibitors, which shows great potential for point-of-care testing, clinical diagnosis, and drug discovery.

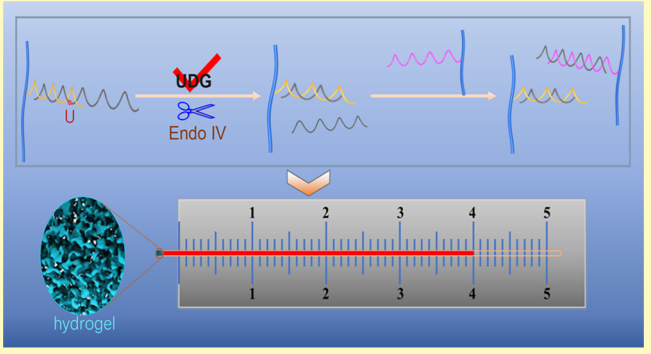

KEYWORDS: *distance-based detection, uracil-DNA glycosylase, DNA hydrogel, membrane filtration, capillary tube*

Maintaining genetic integrity and stability is pivotal for organisms.[1−3] However, deoxyribonucleic acid (DNA) damage can be induced by various endogenous and exogenous stresses, including radiation, ultraviolet light irradiation, and carcinogens.[4−6] If unrepaired, the impairs may lead to gene mutations and the development of many diseases.[7,8] The base-excision repair pathway is an important DNA repair mechanism, which is initiated by DNA glycosylases.[7,9,10] Uracil-DNA glycosylase (UDG) can recognize a mutated uracil base gene in the DNA and cleave the glycosidic bond, generating an apurinic/apyrimidinic (AP) site for further process to restore the original state of DNA.[11−14] The abnormal level of UDG is closely related to many human diseases, such as human immunodeficiency, cancer, bloom syndrome, and so on.[15−17] Therefore, developing sensitive detection of UDG is significant for clinical diagnosis, biomedical research, and drug discovery.[18−20]

Conventionally, gel electrophoresis coupled with the radioisotope ^{32}P-labeled assay is considered to be the gold standard method for UDG analysis.[12] However, this method suffers from some drawbacks, such as radioactive hazard, laborious, and low sensitivity. Alternatively, some nonradioactive methods, including SERS,[21] colorimetric methods,[22] electrochemistry,[23,24] and fluorescent methods,[25] have been proposed, but they suffer from poor sensitivity and complicated operation. In order to improve sensitivity, many efforts have been devoted to developing amplification strategies.[26−30] Nevertheless, these methods require either fluorescently labeled probes, enzyme-assisted amplification reaction, or complicated probe design. Therefore, it is urgently requiring the development of a simple, sensitive, portable, and low-cost method for point-of-care testing (POCT) of the activity of UDG.

Recently, because the inclusion of an analyte-responsive DNA crosslinker allows for gel transition in response to various stimuli including pH,[31] metal ions,[32] and molecules,[33,34] intelligent DNA hydrogel has attracted a lot of attention for sensing, biomimetics, intelligent drug delivery, and biomedical engineering.[35−39] Besides, hydrogels are porous three-dimensional (3D) networks filled with aqueous media, which are

Received: March 27, 2021
Accepted: May 20, 2021
Published: May 28, 2021

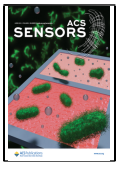

https://doi.org/10.1021/acssensors.1c00624
ACS Sens. 2021, 6, 2395−2402

capable of encapsulating macromolecules[40,41] and separation process.[42] Conventional detection methods based on DNA hydrogel rely on target-induced crosslinker disruption, resulting in gel-to-sol transition and release of encapsulated species. However, most of the reported methods are carried out by encapsulating cargoes in the hydrogel,[40,41] and few reports are used for the detection of biological macromolecules.[43] Therefore, developing a facile, equipment-free, and universal platform for sensitive detection of biomacromolecules based on load-free DNA hydrogel is of great importance for biosensor and clinical research.

Herein, a simple distance readout device was developed for the detection of UDG activity based on load-free DNA hydrogel, integrating a UDG-responsive DNA-linker for bridging polyacrylamide chains with a capillary tube as a signal output device. Prior to the hydrogel construction, UDG reacted with the U strand (sU) and the polyacrylamide left the DNA strand (p-sL) duplex in the liquid system, solving the problem of low activity of the enzyme for the substrate in the hydrogel. In the presence of UDG, the uracil base in sU was recognized and then excised by Endo IV, resulting in the occurrence of some voids and increase in mesh size in the hydrogel. Taking advantage of the membrane filtration technique which is closely related to the mesh size of the hydrogel, quantitative detection of UDG was achieved by reading the distance of the solution in the capillary tube. It should be noted that the detection process is simple: (1) the UDG-treated p-sL and sU complex was mixed with the polyacrylamide right DNA strand (p-sR) for constructing DNA hydrogel and (2) the heat-treated DNA hydrogel was plugged at one end of the tube and horizontally immersed into the red indicator solution for 20 min. Moreover, this method can be utilized for inhibitor screening and detection in cell extracts. Furthermore, distance readout avoids the requirement of equipment, holding considerable promise in POCT and onsite analysis.

■ ASSOCIATED CONTENT

Materials and Reagents. Ammonium persulfate (APS) and tetramethylethylenediamine (TEMED) were purchased from Sigma-Aldrich (St. Louis, MO, U.S.A.). UDG, 10× UDG reaction buffer [200 mM Tris-HCl, 10 mM ethylenediaminetetraacetic acid (EDTA), and 10 mM dithiothreitol (DTT), pH 8.0], Endo IV, uracil glycosylase inhibitor (UGI), formamidopyrimidine [fapy]-DNA glycosylase (Fpg), Nt.BbvCI, and bovine serum albumin (BSA) were purchased from New England Biolabs (Ipswich, MA, U.S.A.). The 6× gel loading buffer and the 20 bp DNA ladder were obtained from Takara Biotechnology Co., Ltd. (Dalian, China). All of the oligonucleotides shown in Table S1, Trizma hydrochloride buffer (Tris-HCl, 1 M, pH 8.0), sodium chloride (NaCl), and the 4S Red Plus nucleic acid stain, were obtained from Sangon Biotech Co., Ltd. (Shanghai, China). Carmine power (red food dye) was purchased from Shanghai Aladdin Bio-Chem Technology Co., Ltd. (Shanghai, China). Capillary tubes (0.3 mm) were purchased from Suzhou City Crystal Glass Co., Ltd. (Suzhou, China). All reagents were of analytical grade and used without any further purification. The Milli-Q water with a resistivity of 18.2 MΩ·cm was used in the experiment.

Polyacrylamide Gel Electrophoresis Analysis. To verify the cleaving reaction of the proposed assay, the reactants and products were analyzed by 12% nondenaturing polyacrylamide gel electrophoresis (PAGE) in 1× TBE buffer (pH 8.3, 90 mM Tris-HCl, 90 mM boric acid, and 2 mM EDTA) at a 120 V constant voltage for 80 min. The gel was stained with Nucleic Acid Stain and photographed by using a Gel Doc EZ Imaging System (Bio-Rad, U.S.A.).

Preparation of Polyacrylamide−DNA Conjugates. The polyacrylamide−DNA conjugates were prepared according to reported work.[33] Briefly, the stock solutions of 500 μM acrydite-DNA right strand (Ac-sR) and acrydite-DNA left strand (Ac-sL) were, respectively, mixed with 4% acrylamide monomer aqueous solution, and oxygen was removed using a deaerator for 10 min. Then, the tubes were quickly put in the deaerator for 15 min for polymerization after adding1.4% APS and TEMED fresh aqueous solutions. After polyreaction, the products were purified by 100 kDa Amicon ultracentrifugal filters (Merck Millipore, Darmstadt, Germany) and obtained the concentrated polymer solutions (p-sL and p-sR). The obtained polymers were stored at 4 °C for further use.

Procedures of the UDG Assay and Inhibition Study. The detection of UDG activity took place in the following steps. First, in 5 μL of 1× UDG buffer (added 50 mM NaCl), the p-sL(250 μM) and sU (250 μM) mixed solution was incubated with various activities of UDG at 37 °C for 60 min in the presence of Endo IV (1 U). It is worth noting that 250 μM of p-sL was used in the UDG reaction, which could reduce the entanglement of polymer chains at high concentration and improve the UDG reaction for DNA on polyacrylamide. After the UDG reaction, the systems were put in the vacuum deaerator for 120 min and then added water to obtain 1 μL concentrated solutions. Afterward, p-sR and Milli-Q water were added into the concentrated solutions and made the final volume of the system to 5 μL including 250 μM p-sR, 250 μM p-sL, and 250 μM sU. The mixed solutions in tubes were heated at 70 °C for 1 min, shaken vigorously three times, and cooled down to room temperature to get a homogeneous hydrogel. Then, the corresponding DNA hydrogel (about 0.3 mm thickness) was plugged at one end of the capillary tube via heating based on denaturation and renaturation of DNA and horizontally immersed in 20 μL of red indicator solution (20 mM Tris-HCl, 100 mM NaCl, and 1% m/v carmine, pH 8.0) at 35 °C for 20 min. Finally, the capillary tube was taken out and fixed on the customized calibrated scale. The activity of UDG was detected by recording the length of the red solution in the capillary tube.

For the UDG inhibition study, UDG at a fixed activity of 0.5 mU/mL was incubated with various concentrations of UGI for 10 min at 37 °C before the addition of the DNA substrate. Then, the incubated solutions were detected by the capillary sensor as described above.

Cell Culture and Real Sample Detection. Human cervical carcinoma cell line (Hela) cells were cultured in Dulbecco's modified Eagle's medium (Gibco, U.S.A.), which were supplemented with 10% fetal bovine serum (Gibco, U.S.A.) and 1% penicillin−streptomycin (Gibco, U.S.A.). The cells were cultured at 37 °C in a humidified atmosphere containing 5% CO_2 and 95% air. During the exponential phase of growth, Hela cells were collected with trypsinization and washed with phosphate buffer saline (PBS, pH 7.4, Gibco, U.S.A.). The cellular active protein was extracted by using the animal cell active protein extraction kit (Sangon, China) according to the operating instruction. The obtained protein supernatant was stored at −80 °C for further assay. The UDG activity in Hela cells was detected following the standard procedure described.

https://doi.org/10.1021/acssensors.1c00624
ACS Sens. 2021, 6, 2395−2402

Scheme 1. (a) Schematic Representation of UDG Activity Detection Based on DNA Hydrogel and (b) Biosensing Illustration of UDG via a Capillary Tube on the Ruler

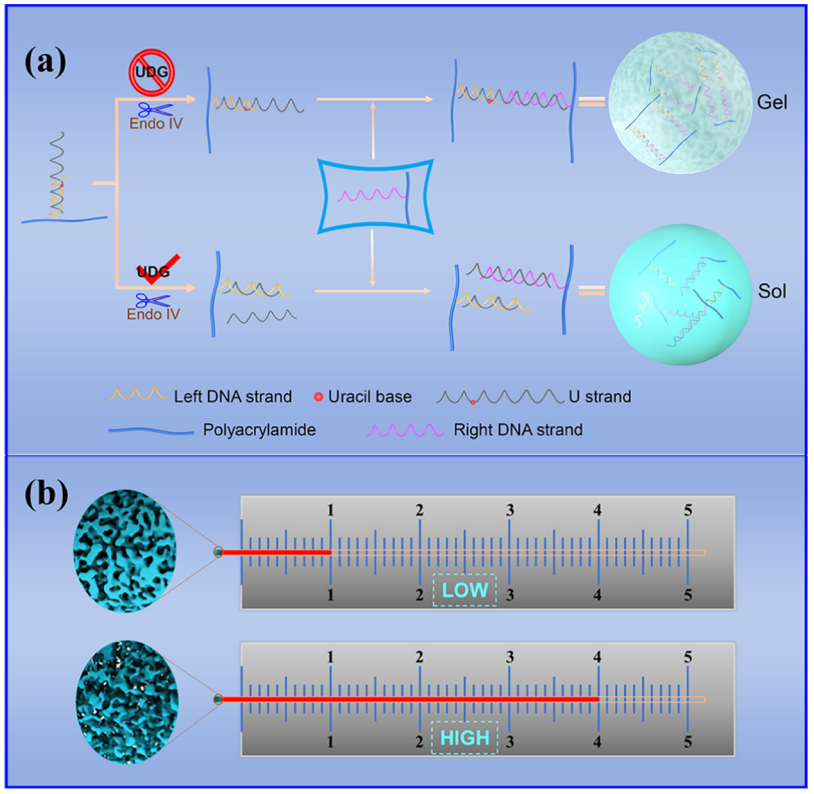

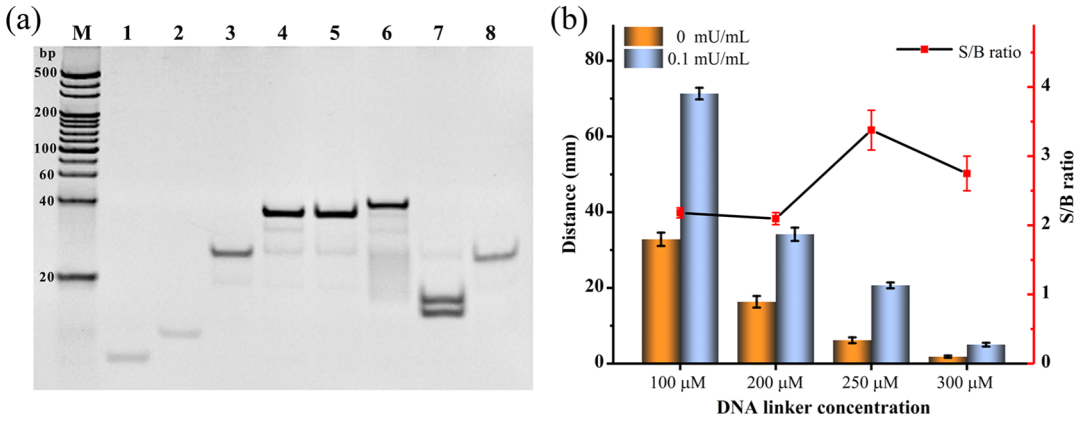

Figure 1. (a) Nondenaturing PAGE to prove the feasibility of the cleavage effect. Lane M: DNA ladder marker; lane 1: left DNA strand; lane 2: right DNA strand; lane 3: U strand; lane 4: sL + sR + sU (=Uz); lane 5: lane 4 + Endo IV; lane 6: lane 4 + UDG; lane 7: lane 4 + UDG + Endo IV; and lane 8: sU + UDG + Endo IV. (b) Optimization of DNA concentration in the hydrogel. Left *y*-axis: distance signals were obtained from the 0.1 mU/mL UDG (blue column) and 0 mU/mL control group (brown column). Right *y*-axis: the corresponding *S*/*B* ratios of different systems. The molar ratio was sR/sL/sU = 1:1:1, and the sU crosslinker at four concentrations: 100, 200, 250, and 300 μM. The Na^+ concentration in the indicator solution was 100 mM. The distance was recorded after being incubated at 30 °C for 20 min. The data point is the average of three measurements (n = 3), and error bars represent the standard deviation.

RESULTS AND DISCUSSION

Principle of the Strategy for the UDG Assay. The working principle of the visual biosensor for the detection of UDG based on DNA hydrogel is illustrated in Scheme 1. In the absence of UDG, the U strand modified with one uracil base (responsive site) is stable and can simultaneously hybridize with DNA strands of the p-sR and p-sL chains, generating the homogeneous DNA hydrogel. The DNA secondary structure of the hydrogel is shown in Figure S1a. However, target UDG can specifically recognize the uracil base in sU and remove it by cleaving the *N*-glycosidic bond between the uracil and the deoxyribose sugar of the DNA substrate, forming an apurinic−apyrimidinic (AP) site.[13] The AP site can be cleaved with the assistance of Endo IV,[28] resulting in the cleavage effect for sU in the duplex substrate, and the partial sU fragment in a free state. The detailed pathway of cleavage reactions is shown in Figure S1b. Meanwhile, sU loses the function of the crosslinker to bind to two polymer chains, resulting in the decrease of crosslink density and the increase of mesh size of the hydrogel.

https://doi.org/10.1021/acssensors.1c00624
ACS Sens. 2021, 6, 2395−2402

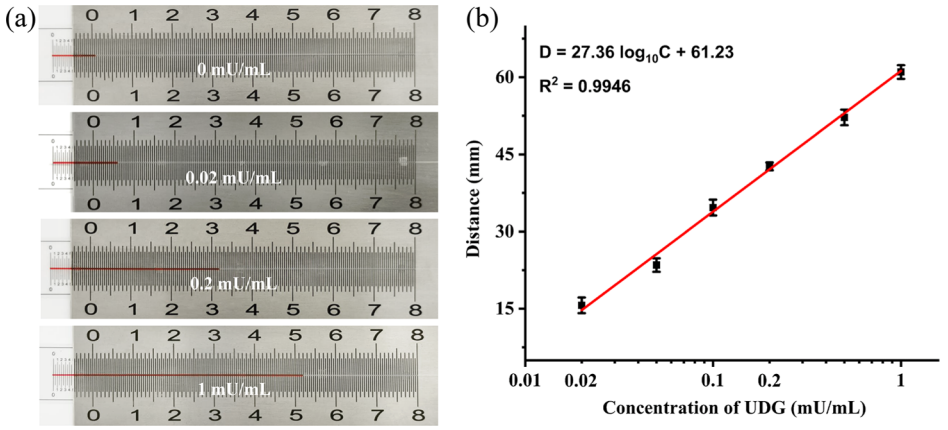

Figure 2. (a) Photographs of the proposed strategy for detecting different concentrations of UDG. (b) Liner relationship between the distance and the logarithm of the UDG concentration in the range from 0.02 to 1 mU/mL. The error bars represent the standard deviation of three measurements (n = 3).

After the target UDG-treated process, the hydrogel occurs to form an inhomogeneous hydrogel with more voids compared with that in the absence of UDG. With the increase in UDG concentration, more molecules could quickly flow into the tube due to the presence of more and larger voids in the hydrogel and the increase of mesh size. The scanning electron microscopy (SEM) images of the hydrogel in the absence and presence of UDG are shown in Figure S2a,b, revealing that the hydrogel is a 3D microporous structure and the UDG-treated hydrogel has larger pores. The photographs of the biosensor before and after being immersed in the red indicator solution are shown in Figure S2c,d, indicating that the red indicator solution would flow through the hydrogel membrane and then into the capillary tube during immersion. Therefore, the separation performance is based on the mesh size of the DNA hydrogel, which can be affected by UDG activity. In summary, by reading the distance of the red indicator solution in the capillary tube, the macromolecule UDG activity can be visually and directly quantified without signal amplification and complex operations.

Feasibility of the Proposed Method. To investigate the feasibility of the UDG-initiated excision reaction, DNA strands utilized in this proposed assay and reaction products were characterized by nondenaturing PAGE. As illustrated in Figure 1a, lane 1, lane 2, and lane 3 show the bands of right DNA strand (sR), left DNA strand (sL), and sU respectively. Lane 4 shows the gel band of the hybridization products of sR, sL, and sU (named Uz), which is bridged by sU. Lane 5 and lane 6 show the products of Uz treated with Endo IV and UDG, respectively, and no DNA fragment below the Uz band is observed, indicating that Endo IV and UDG would not individually initiate the cleavage effect for the sU crosslinker. In contrast, in the presence of UDG and Endo IV for the Uz system, two new bands below 20 bp DNA marker are observed (Figure 1a, lane 7), which are comparable to the two broken fragments of Uz. This result indicates that UDG can specially recognize responsive uracil base and induce the cleavage reaction with the assistance of Endo IV. The products of sU single strands incubated with UDG and Endo IV are observed in lane 8, indicating that the cleavage effect on single-stranded DNA (ssDNA) is very weaker than the double-stranded DNA (dsDNA) shown in lane 7. These results demonstrate that UDG could trigger the excision reaction, and thus, the proposed strategy is feasible for target UDG detection.

Optimization of Experimental Conditions. To obtain the optimal performance, the experimental conditions, including the DNA concentration in the hydrogel, Na^+ concentration in the red indicator solution, and the measuring temperature, were systematically investigated. Membrane filtration relies on the mesh size of the hydrogel and can be influenced by some factors including solute concentration and temperature.[42,44] The mesh size of hydrogel depends on many factors, such as crosslinker and polymer concentrations and stimulus.[44] The influence of DNA concentration in the hydrogel was first investigated. As shown in Figure 1b, the signal-to-blank (S/B) ratio (S represents the distance signal of the experimental group and B represents the signal of the control group) reaches the maximum at a concentration of 250 μM ranging from 100 to 300 μM, indicating that 250 μM of sU at a ratio of 1:1:1 (p-sR/p-sL/sU) is the optimal concentration. During testing, the amount of Na^+ and measuring temperature were optimized. As illustrated in Figure S3, with the increasing concentration of Na^+, the distance signal increases, but the S/B ratio decreases when the concentration of Na^+ reaches 100 mM. Thus, the indicator solution including 100 mM Na^+ was chosen as the optimal concentration. The influence of the measuring temperature upon the UDG detection is shown in Figure S4, and the highest value of S/B ratio is obtained at 35 °C. Therefore, 250 μM sU, 100 mM Na^+, and 35 °C were used in the following analysis.

Visual Detection of UDG via a Capillary Tube. Under optimized conditions, visual detection of UDG based on membrane filtration of DNA hydrogel was performed by reading the distance of the indicator solution in the capillary tube. Treated with a series of concentrations of UDG, sU was used for the synthesis of DNA hydrogel samples, which acts as a signal converter for UDG detection. As shown in Figures 2a and S5, photographs of the sensing systems indicate that the distance of the red indicator solution in the capillary tube can be clearly observed, and the distance increases as the concentration of UDG increases. In the presence of high concentration of UDG, the liquid diffusion is quicker than the low concentration system. The corresponding linear relationship between the distance signal and the logarithm of the UDG concentration in the range from 0.02 to 1 mU/mL is shown in Figure 2b. The correlation equation is D (mm) = 27.36 $\log_{10}C$ + 61.23 with a correlation coefficient of 0.9946, where D is the distance signal and C is the concentration of UDG (mU/mL).

https://doi.org/10.1021/acssensors.1c00624
ACS Sens. 2021, 6, 2395−2402

The minimum detective concentration (MDC) of this method is 0.02 mU/mL.

To compare the analysis performance between the proposed method and other reported methods,[21−23,25−30] a study shown in Table S2 is carried out on an operational strategy, required materials, linear range, and MDC. In comparison with the reported colorimetric assay (8 mU/mL),[22] as low as 0.02 mU/mL of UDG can be detected by visualizing the distance of the red indicator solution in the capillary, and the sensitivity has enhanced by 400-fold. The proposed visualization method is not only sensitive but also does not require specialized equipment such as fluorometer, Raman spectrometer, and electrochemical workstation. The MDC of this method is comparable and even superior to amplification strategies,[28−30] which need fine design, additional enzyme, and fluorescently labeled probe. The improved sensitivity may be attributed to the specific excision reaction initiated by UDG, resulting in the increase of mesh size of the hydrogel, and the highly efficient membrane filtration of the DNA hydrogel. In addition, this proposed method possesses several significant advantages: (1) with only a capillary tube, visual detection of UDG can be achieved without the bulky instruments; (2) operation is extremely simple, and the signal is easier to read than the colorimetric method; and (3) this method is low-cost without amplification techniques, quencher−fluorophore DNA probes, and enzyme-trapped hydrogel. Overall, the proposed method not only provides a sensitive way for visual detection of the target but also could be extended for other biomacromolecule detection by adjusting the target-responsive DNA in the hydrogel.

Selectivity of the UDG Assay. To evaluate the specificity of the proposed method, other interferences were used, including formamidopyrimidine [fapy]-DNA glycosylase (Fpg, also known as 8-oxoguanine DNA glycosylase), Nt.BbvCI, and BSA. BSA cannot excise the damaged uracil bases in DNA substrates.[12] Fpg can recognize and catalyze the excision of 8-oxoguanine, which is one of the most abundant DNA lesions.[45] The nicking endonuclease of Nt.BbvCI can cleave the specific DNA sequence of one DNA strand in double-stranded DNA.[46] Theoretically speaking, these enzymes cannot break the DNA linker to induce the degradation of the DNA hydrogel. As shown in Figure 3, neglectable signals compared to the reaction buffer system (Figure 3, violet column) are detected in the presence of Fpg, Nt.BbvCI, and BSA. However, a significant signal in the detection of UDG is observed (Figure 3, red column). The corresponding smart phone photographs of the biosensing systems are shown in Figure S6. These results demonstrate that this method has high specificity for UDG detection.

UDG Inhibition Study. In order to demonstrate the feasibility of the proposed biosensor for UDG inhibition assay, UGI was investigated. UGI protein from *Bacillus subtilis* bacteriophage PBS1 has a tight binding affinity to UDG in 1:1 M stoichiometry and thus potently blocks removal of uracil in DNA.[47,48] As shown in Figure 4, the relative activity of UDG gradually decreases with the increasing concentration of UGI in the range of 0−5 mU/mL. Based on the plot of the relative activity of UDG versus UGI concentration, the half maximal inhibitory concentration (IC_{50}) value was calculated to be 0.511 mU/mL, indicating that UGI has a strong inhibitory effect on UDG. This result demonstrates that the proposed strategy can be utilized for screening the UDG inhibitors, which is of great importance to drug discovery.

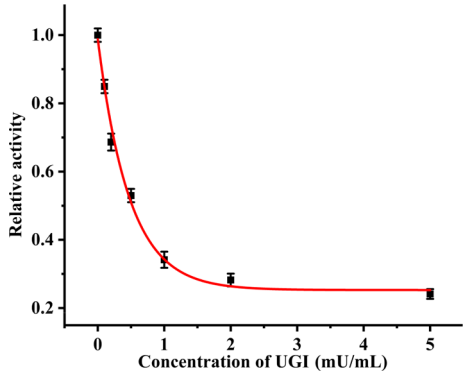

Figure 4. Relative activity of UDG in response to increasing concentrations of UGI ranging from 0 to 5 mU/mL. The UDG concentration is 0.5 mU/mL.

Detection of Cellular UDG Activity. To evaluate the applicability of our strategy for complex biosamples, UDG activity in Hela cells was detected under the optimized experimental conditions. As shown in Figure 5, the obvious signal is observed in cell extracts (brown column), while the distance signal decreases to the level of the control group (blank column) in the presence of excess UGI (2 mU/mL, blue column). Furthermore, UDG (0.3 mU/mL) spiked into

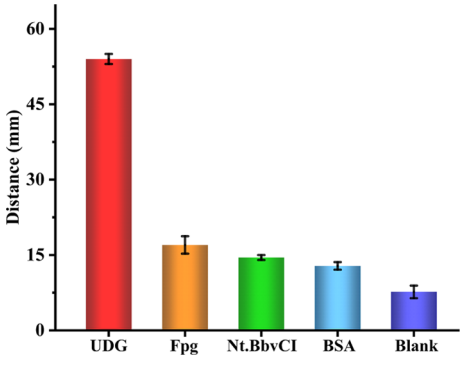

Figure 3. Distances of the biosensing systems in response to 0.5 mU/mL UDG, 0.5 mU/mL Fpg, 0.5 mU/mL Nt.BbvCI, 10 ng/mL BSA, and the reaction buffer (blank group). Error bars indicate standard deviation (n = 3).

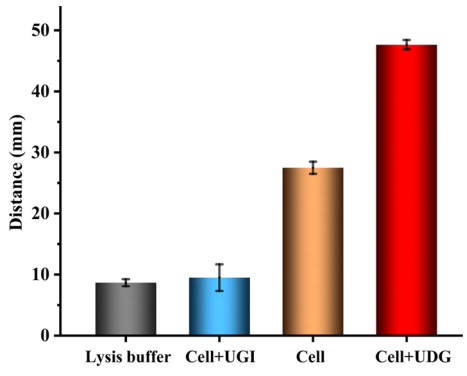

Figure 5. Distances of the biosensing systems in the presence of lysis buffer (blank column), cell + UGI (blue column), cell (brown column), and cell + UDG (red column). Error bars indicate standard deviation (n = 3).

https://doi.org/10.1021/acssensors.1c00624
ACS Sens. 2021, 6, 2395−2402

the cell extract was determined to be 0.26 mU/mL with a recovery of 86.7%. Meanwhile, the relative standard deviation was 4.5% (n = 3), indicating that the proposed biosensor performed an acceptable reproducibility for detecting UDG in the real sample. Figure S7 shows the real-time photographs of the sensing systems observed by the naked eye. These results confirm that this simple method is reliable for visual detection of UDG in complex biosamples, holding great promise for clinical diagnosis.

CONCLUSIONS

In summary, a facile method using membrane filtration of DNA hydrogel for visual detection of UDG via a capillary tube as a distance-based analytical device was developed. This method exhibits significant advantages: (1) by integration of the specific recognition ability of UDG and efficient filtration of DNA hydrogel membrane, this method shows excellent sensitivity with the detection of UDG as low as 0.02 mU/mL, which is superior to reported amplification strategies.[28,29] (2) This method demonstrates the detection of a biomacromolecule based on a load-free DNA hydrogel, which may be generally applicable for sensing of various targets by incorporation of the appropriate target-responsive nucleotide sequence in the hydrogel. (3) The approach avoids complicated processes, such as encapsulating enzymes in the hydrogel,[41] and the distance-based signal provides a convenient means to quantify enzyme activity by the naked eye, which can be useful for POCT. Therefore, on the basis of simple, cost-effective, ease of use, universal, and sensitivity, this proposed biosensor holds great potential for POCT in low-resource settings, clinical diagnosis, and biomedical study.

ASSOCIATED CONTENT

Supporting Information

The Supporting Information is available free of charge at https://pubs.acs.org/doi/10.1021/acssensors.1c00624.

Sequences of the oligonucleotides; comparison of the proposed method with other reported methods; DNA structure of the hydrogel and pathway of cleavage reactions; SEM images of the hydrogel and photographs of the sensor; optimization of several experimental conditions; and photographs of several testing systems (PDF)

AUTHOR INFORMATION

Corresponding Author

Yongqiang Wen − *Beijing Key Laboratory for Bioengineering and Sensing Technology, Daxing Research Institute, School of Chemistry and Biological Engineering, University of Science and Technology Beijing, Beijing 100083, People's Republic of China*; orcid.org/0000-0002-1924-4166; Email: wyq_wen@ustb.edu.cn

Authors

Chao Jiang − *Beijing Key Laboratory for Bioengineering and Sensing Technology, Daxing Research Institute, School of Chemistry and Biological Engineering, University of Science and Technology Beijing, Beijing 100083, People's Republic of China*

Fangfang Wang − *Beijing Key Laboratory for Bioengineering and Sensing Technology, Daxing Research Institute, School of Chemistry and Biological Engineering, University of Science and Technology Beijing, Beijing 100083, People's Republic of China*

Kexin Zhang − *Beijing Key Laboratory for Bioengineering and Sensing Technology, Daxing Research Institute, School of Chemistry and Biological Engineering, University of Science and Technology Beijing, Beijing 100083, People's Republic of China*

Tiantian Min − *Beijing Key Laboratory for Bioengineering and Sensing Technology, Daxing Research Institute, School of Chemistry and Biological Engineering, University of Science and Technology Beijing, Beijing 100083, People's Republic of China*

Desheng Chen − *Beijing Key Laboratory for Bioengineering and Sensing Technology, Daxing Research Institute, School of Chemistry and Biological Engineering, University of Science and Technology Beijing, Beijing 100083, People's Republic of China*

Complete contact information is available at: https://pubs.acs.org/10.1021/acssensors.1c00624

Author Contributions

All authors have given approval to the final version of the manuscript.

Notes

The authors declare no competing financial interest.

ACKNOWLEDGMENTS

This work was financially supported by the National Natural Science Foundation of China (21975019), the National Key Research and Development Program of China (2018YFD0401302), the Beijing Science Technology New Star Cross Subject (2018019), and the Fundamental Research Funds for the Central Universities and USTB.

ABBREVIATIONS2-COL

UDG, uracil-DNA glycosylase; Endo IV, endonuclease IV; sU, U strand; p-sL, polyacrylamide left DNA strand; p-sR, polyacrylamide right DNA strand; Ac-sR, acrydite-DNA right strand; Ac-sL, acrydite-DNA left strand.

REFERENCES

(1) Piazza, A.; Wright, W. D.; Heyer, W.-D. Multi-invasions Are Recombination Byproducts that Induce Chromosomal Rearrangements. *Cell* **2017**, *170*, 760−773.

(2) Jiménez-Martín, A.; Saugar, I.; Joseph, C. R.; Mayer, A.; Lehmann, C. P.; Szakal, B.; Branzei, D.; Tercero, J. A. The Mgs1/WRNIP1 ATPase is Required to Prevent a Recombination Salvage Pathway at Damaged Replication Forks. *Sci. Adv.* **2020**, *6*, No. eaaz3327.

(3) Ray Chaudhuri, A.; Nussenzweig, A. The Multifaceted Roles of PARP1 in DNA Repair and Chromatin Remodelling. *Nat. Rev. Mol. Cell Biol.* **2017**, *18*, 610−621.

(4) David, S. S.; O'Shea, V. L.; Kundu, S. Base-Excision Repair of Oxidative DNA Damage. *Nature* **2007**, *447*, 941−950.

(5) Lord, C. J.; Ashworth, A. The DNA Damage Response and Cancer Therapy. *Nature* **2012**, *481*, 287−294.

(6) Gaillard, H.; Aguilera, A. Transcription as a Threat to Genome Integrity. *Annu. Rev. Biochem.* **2016**, *85*, 291−317.

(7) Chaim, I. A.; Nagel, Z. D.; Jordan, J. J.; Mazzucato, P.; Ngo, L. P.; Samson, L. D. In Vivo Measurements of Interindividual Differences in DNA Glycosylases and APE1 Activities. *Proc. Natl. Acad. Sci. U.S.A.* **2017**, *114*, E10379−E10388.

(8) Aguilera, A.; García-Muse, T. Causes of Genome Instability. *Annu. Rev. Genet.* **2013**, *47*, 1−32.

(9) Mullins, E. A.; Rodriguez, A. A.; Bradley, N. P.; Eichman, B. F. Emerging Roles of DNA Glycosylases and the Base Excision Repair Pathway. *Trends Biochem. Sci.* **2019**, *44*, 765−781.
(10) Sarno, A.; Lundbæk, M.; Liabakk, N. B.; Aas, P. A.; Mjelle, R.; Hagen, L.; Sousa, M. M. L.; Krokan, H. E.; Kavli, B. Uracil-DNA Glycosylase UNG1 Isoform Variant Supports Class Switch Recombination and Repairs Nuclear Genomic Uracil. *Nucleic Acids Res.* **2019**, *47*, 4569−4585.
(11) Ahn, W.-C.; Aroli, S.; Kim, J.-H.; Moon, J. H.; Lee, G. S.; Lee, M.-H.; Sang, P. B.; Oh, B.-H.; Varshney, U.; Woo, E.-J. Covalent Binding of Uracil DNA Glycosylase UdgX to Abasic DNA upon Uracil Excision. *Nat. Chem. Biol.* **2019**, *15*, 607−614.
(12) Li, C.-C.; Chen, H.-Y.; Hu, J.; Zhang, C.-Y. Rolling Circle Amplification-Driven Encoding of Different Fluorescent Molecules for Simultaneous Detection of Multiple DNA Repair Enzymes at the Single-Molecule Level. *Chem. Sci.* **2020**, *11*, 5724−5734.
(13) Prorok, P.; Alili, D.; Saint-Pierre, C.; Gasparutto, D.; Zharkov, D. O.; Ishchenko, A. A.; Tudek, B.; Saparbaev, M. K. Uracil in Duplex DNA is a Substrate for the Nucleotide Incision Repair Pathway in Human Cells. *Proc. Natl. Acad. Sci. U.S.A.* **2013**, *110*, E3695−E3703.
(14) Baños-Sanz, J. I.; Mojardín, L.; Sanz-Aparicio, J.; Lázaro, J. M.; Villar, L.; Serrano-Heras, G.; González, B.; Salas, M. Crystal Structure and Functional Insights into Uracil-DNA Glycosylase Inhibition by Phage Phi29 DNA Mimic Protein p56. *Nucleic Acids Res.* **2013**, *41*, 6761−6773.
(15) Xiang, Y.; Lu, Y. Expanding Targets of DNAzyme-Based Sensors Through Deactivation and Activation of DNAzymes by Single Uracil Removal: Sensitive Fluorescent Assay of Uracil-DNA Glycosylase. *Anal. Chem.* **2012**, *84*, 9981−9987.
(16) Seal, G.; Brech, K.; Karp, S. J.; Cool, B. L.; Sirover, M. A. Immunological Lesions in Human Uracil DNA Glycosylase: Association with Bloom Syndrome. *Proc. Natl. Acad. Sci. U.S.A.* **1988**, *85*, 2339−2343.
(17) Chen, X.; Wu, Y.; Cao, G.; Wang, X.; Ji, Z.; Huo, D.; Xu, F.; Hou, C. A Methodology for Ultrasensitive Detection of Sequence-Specific DNA or Uracil-DNA Glycosylase Activity. *ACS Sens.* **2020**, *5*, 1615−1623.
(18) Li, G.; Henry, S. A.; Liu, H.; Kang, T.-S.; Nao, S.-C.; Zhao, Y.; Wu, C.; Jin, J.; Zhang, J.-T.; Leung, C.-H.; Wai Hong Chan, P.; Ma, D.-L. A Robust Photoluminescence Screening Assay Identifies Uracil-DNA Glycosylase Inhibitors Against Prostate Cancer. *Chem. Sci.* **2020**, *11*, 1750−1760.
(19) Xu, X.; Zhang, P.; Zhang, R.; Zhang, N.; Jiang, W. A DNA Walker Powered by Endogenous Enzymes for Imaging Uracil-DNA Glycosylase Activity in Living Cells. *Chem. Commun.* **2019**, *55*, 6026−6029.
(20) Wang, L.-J.; Ren, M.; Zhang, Q.; Tang, B.; Zhang, C.-Y. Excision Repair-Initiated Enzyme-Assisted Bicyclic Cascade Signal Amplification for Ultrasensitive Detection of Uracil-DNA Glycosylase. *Anal. Chem.* **2017**, *89*, 4488−4494.
(21) Wang, H.; Cui, Y.; Wang, J.; Liu, S.; Zhang, X.; Song, X.; Wang, Y.; Huang, J.; Yu, J. A Facile and Robust SERS Platform for Highly Sensitive and Reproducible Detection of Uracil-DNA Glycosylase Using Target-Activated Plasmonic Coupling. *Sens. Actuators, B* **2019**, *287*, 535−543.
(22) Nie, H.; Wang, W.; Li, W.; Nie, Z.; Yao, S. A Colorimetric and Smartphone Readable Method for Uracil-DNA Glycosylase Detection Based on the Target-Triggered Formation of G-Quadruplex. *Analyst* **2015**, *140*, 2771−2777.
(23) Liu, T.; Cui, L.; Li, D.; Gao, W.; Wu, L.; Zhang, X. An Enzyme-Free and Substrate-Free Electrochemical Biosensor with Robust Porphyrin-Based Covalent-Linked Nanomaterial as Nanoelectrocatalyst and Efficient Support for Sensitive Detection of Uracil-DNA Glycosylase. *Biosens. Bioelectron.* **2020**, *154*, 112014.
(24) Zhao, M.-H.; Cui, L.; Sun, B.; Wang, Q.; Zhang, C.-Y. Low-Background Electrochemical Biosensor for One-Step Detection of Base Excision Repair Enzyme. *Biosens. Bioelectron.* **2020**, *150*, 111865.
(25) Zhang, X. F.; Li, N.; Ling, Y.; Tang, L.; Li, N. B.; Luo, H. Q. Linked Bridge Hybridizing-Induced Split G-Quadruplex DNA Machine and Its Application to Uracil-DNA Glycosylase Detection. *Sens. Actuators, B* **2018**, *255*, 2589−2594.
(26) Ren, R.; Shi, K.; Yang, J.; Yuan, R.; Xiang, Y. DNA Three Way Junction-Mediated Recycling Amplification for Sensitive Electrochemical Monitoring of Uracil-DNA Glycosylase Activity and Inhibition. *Sens. Actuators, B* **2018**, *258*, 783−788.
(27) Wang, J.; Pan, M.; Wei, J.; Liu, X.; Wang, F. A C-HCR Assembly of Branched DNA Nanostructures for Amplified Uracil-DNA Glycosylase Assays. *Chem. Commun.* **2017**, *53*, 12878−12881.
(28) Du, Y.-C.; Cui, Y.-X.; Li, X.-Y.; Sun, G.-Y.; Zhang, Y.-P.; Tang, A.-N.; Kim, K.; Kong, D.-M. Terminal Deoxynucleotidyl Transferase and T7 Exonuclease-Aided Amplification Strategy for Ultrasensitive Detection of Uracil-DNA Glycosylase. *Anal. Chem.* **2018**, *90*, 8629−8634.
(29) Zhang, X. F.; Li, N.; Ling, Y.; Li, N. B.; Luo, H. Q. Sensitive Detection of Active Uracil-DNA Glycosylase via an Exonuclease III-Assisted Cascade Multi-Amplification Fluorescence DNA Machine. *Sens. Actuators, B* **2018**, *271*, 9−14.
(30) Zhang, P.; Wang, L.; Zhao, H.; Xu, X.; Jiang, W. Self-Primer and Self-Template Recycle Rolling Circle Amplification Strategy for Sensitive Detection of Uracil-DNA Glycosylase Activity. *Anal. Chim. Acta* **2018**, *1001*, 119−124.
(31) Liao, W.-C.; Lilienthal, S.; Kahn, J. S.; Riutin, M.; Sohn, Y. S.; Nechushtai, R.; Willner, I. pH- and Ligand-Induced Release of Loads from DNA-Acrylamide Hydrogel Microcapsules. *Chem. Sci.* **2017**, *8*, 3362−3373.
(32) Dave, N.; Chan, M. Y.; Huang, P.-J. J.; Smith, B. D.; Liu, J. Regenerable DNA-Functionalized Hydrogels for Ultrasensitive, Instrument-Free Mercury(II) Detection and Removal in Water. *J. Am. Chem. Soc.* **2010**, *132*, 12668−12673.
(33) Li, Y.; Ma, Y.; Jiao, X.; Li, T.; Lv, Z.; Yang, C. J.; Zhang, X.; Wen, Y. Control of Capillary Behavior Through Target-Responsive Hydrogel Permeability Alteration for Sensitive Visual Quantitative Detection. *Nat. Commun.* **2019**, *10*, 1036.
(34) Si, Y.; Xu, L.; Wang, N.; Zheng, J.; Yang, R.; Li, J. Target MicroRNA-Responsive DNA Hydrogel-Based Surface-Enhanced Raman Scattering Sensor Arrays for MicroRNA-Marked Cancer Screening. *Anal. Chem.* **2020**, *92*, 2649−2655.
(35) Li, F.; Lyu, D.; Liu, S.; Guo, W. DNA Hydrogels and Microgels for Biosensing and Biomedical Applications. *Adv. Mater.* **2020**, *32*, 1806538.
(36) Song, P.; Ye, D.; Zuo, X.; Li, J.; Wang, J.; Liu, H.; Hwang, M. T.; Chao, J.; Su, S.; Wang, L.; Shi, J.; Wang, L.; Huang, W.; Lal, R.; Fan, C. DNA Hydrogel with Aptamer-Toehold-Based Recognition, Cloaking, and Decloaking of Circulating Tumor Cells for Live Cell Analysis. *Nano Lett.* **2017**, *17*, 5193−5198.
(37) Shao, Y.; Jia, H.; Cao, T.; Liu, D. Supramolecular Hydrogels Based on DNA Self-Assembly. *Acc. Chem. Res.* **2017**, *50*, 659−668.
(38) Dong, Y.; Yao, C.; Zhu, Y.; Yang, L.; Luo, D.; Yang, D. DNA Functional Materials Assembled from Branched DNA: Design, Synthesis, and Applications. *Chem. Rev.* **2020**, *120*, 9420−9481.
(39) Kahn, J. S.; Hu, Y.; Willner, I. Stimuli-Responsive DNA-Based Hydrogels: From Basic Principles to Applications. *Acc. Chem. Res.* **2017**, *50*, 680−690.
(40) Mao, X.; Chen, G.; Wang, Z.; Zhang, Y.; Zhu, X.; Li, G. Surface-Immobilized and Self-Shaped DNA Hydrogels and Their Application in Biosensing. *Chem. Sci.* **2018**, *9*, 811−818.
(41) Wei, X.; Tian, T.; Jia, S.; Zhu, Z.; Ma, Y.; Sun, J.; Lin, Z.; Yang, C. J. Microfluidic Distance Readout Sweet Hydrogel Integrated Paper-Based Analytical Device (μDiSH-PAD) for Visual Quantitative Point-of-Care Testing. *Anal. Chem.* **2016**, *88*, 2345−2352.
(42) Shang, W.; Li, X.; Liu, W.; Yue, S.; Li, M.; von Eiff, D.; Sun, F.; An, A. K. Effective Suppression of Concentration Polarization by Nanofiltration Membrane Surface Pattern Manipulation: Numerical Modeling based on LIF Visualization. *J. Membr. Sci.* **2021**, *622*, 119021.
(43) Gao, X.; Li, X.; Sun, X.; Zhang, J.; Zhao, Y.; Liu, X.; Li, F. DNA Tetrahedra-Cross-Linked Hydrogel Functionalized Paper for Onsite

https://doi.org/10.1021/acssensors.1c00624
ACS Sens. 2021, 6, 2395−2402

Analysis of DNA Methyltransferase Activity Using a Personal Glucose Meter. *Anal. Chem.* **2020**, *92*, 4592−4599.
(44) Li, J.; Mooney, D. J. Designing Hydrogels for Controlled Drug Delivery. *Nat. Rev. Mater.* **2016**, *1*, 16071.
(45) Kreppel, A.; Blank, I. D.; Ochsenfeld, C. Base-Independent DNA Base-Excision Repair of 8-Oxoguanine. *J. Am. Chem. Soc.* **2018**, *140*, 4522−4526.
(46) Xie, H.; Wang, Q.; Chai, Y.; Yuan, Y.; Yuan, R. Enzyme-Assisted Cycling Amplification and DNA-Templated in-Situ Deposition of Silver Nanoparticles for the Sensitive Electrochemical Detection of Hg^{2+}. *Biosens. Bioelectron.* **2016**, *86*, 630−635.
(47) Komor, A. C.; Kim, Y. B.; Packer, M. S.; Zuris, J. A.; Liu, D. R. Programmable Editing of a Target Base in Genomic DNA without Double-Stranded DNA Cleavage. *Nature* **2016**, *533*, 420−424.
(48) Nishida, K.; Arazoe, T.; Yachie, N.; Banno, S.; Kakimoto, M.; Tabata, M.; Mochizuki, M.; Miyabe, A.; Araki, M.; Hara, K. Y.; Shimatani, Z.; Kondo, A. Targeted Nucleotide Editing Using Hybrid Prokaryotic and Vertebrate Adaptive Immune Systems. *Science* **2016**, *353*, aaf8729.

https://doi.org/10.1021/acssensors.1c00624
ACS Sens. 2021, 6, 2395−2402